AIAA JOURNAL
Vol. 33, No. 6, June 1995

Thermomechanical Fatigue Life Prediction in Gas Turbine Superalloys: A Fracture Mechanics Approach

David M. Nissley*
United Technologies Corporation, East Hartford, Connecticut 06108

A model is presented that was developed to predict thermomechanical fatigue crack initiation and estimate mode I crack growth of gas turbine hot section gas path superalloys. The model is based on a strain energy density fracture mechanics approach modified to account for thermal exposure and single crystal anisotropy. Thermomechanical fatigue crack initiation and small crack growth is modeled by employing an initial material defect size. Model capability was quantified by applying the model to two hot section gas path superalloys: uncoated MAR-M509 and MCrAlY overlay coated PWA 1480. Thermomechanical fatigue model stresses were obtained from nonlinear finite element analysis of thermomechanical fatigue specimen strain-temperature history. Nonlinear stress–strain behavior was predicted using unified viscoplastic constitutive models. Model thermomechanical fatigue life predictions were in good agreement with observed uniaxial thermomechanical fatigue specimen lives. Thermomechanical fatigue cracking effects captured by the model included coating thickness, single crystal anisotropy, cycle waveshape, dwell, and thermal exposure.

Nomenclature

a	= crack depth
a_0	= initial material defect size
dt	= time increment
da/dN	= crack growth rate
$d\varepsilon^{in}$	= inelastic strain increment
E_{max}	= elastic modulus in the σ_{max} direction and at the σ_{max} temperature
$E_{\langle 111\rangle}$	= elastic modulus in the $\langle 111\rangle$ crystal direction and at the σ_{max} temperature
f	= crystallographic strain energy correction factor
$f_{\langle 111\rangle}$	= factor that resolves σ_{max} into the maximum normal octahedral slip plane stress
J_{eff}	= effective J-integral, an empirical strain energy density fracture mechanics parameter
J_{th}	= threshold J-integral
l	= crack length
N_c	= cycles to initiate a crack through the coating
N_f	= cycles to failure
N_{sc}	= cycles for a coating crack to penetrate 0.254mm deep into the substrate
N_{sp}	= cycles to grow a 0.254 mm deep substrate crack to failure
T	= absolute temperature
T_{max}	= cycle maximum absolute temperature
t_c	= coating thickness
W_e	= elastic strain energy density
W_{eff}^{tot}	= effective total strain energy density
W_p	= plastic strain energy density
β	= crack-boundary-correction factor
ΔJ	= J-integral based on $\Delta\sigma$
ΔJ_e	= elastic portion of ΔJ
ΔJ_p	= plastic portion of ΔJ
$\Delta\sigma$	= stress range
δ	= oxide thickness
σ	= stress
σ_{max}	= maximum stress
σ_{min}	= minimum stress of cycle in which σ_{max} occurs

Received Feb. 15, 1994; revision received Jan. 3, 1995; accepted for publication Jan. 7, 1995. Copyright © 1995 by David M. Nissley. Published by the American Institute of Aeronautics and Astronautics, Inc., with permission.

*Project Engineer, Pratt and Whitney Division.

Introduction

ADVANCED gas turbine operating temperatures subject hot section gas path components to extreme heat loads. Component thermal gradients introduced by the heat loads promote thermomechanical fatigue (TMF) cracking.

Implementation of an accurate TMF life prediction model will improve hot section component design and life cycle costs. The TMF model should be capable of predicting both crack initiation and crack growth. TMF crack initiation is important for rotating hardware such as turbine blades. TMF cracking in static hardware such as turbine vanes and blade tip seals includes both crack initiation and crack growth regimes.

Investigators generally separate fatigue crack initiation from crack growth. Crack initiation is dominated by microscopic effects such as surface finish, microdefects, slip characteristics, and grain size. Crack growth describes long crack behavior in which crack geometry is important. Fatigue crack initiation life modeling traditionally takes the form of a Coffin–Manson relationship, $N = CP^m$ where P is the correlating parameter and C and m are material constants. Crack growth can be described by linear or nonlinear fracture mechanics methods. Typically, a power law formulation is used, $da/dN = AP^b$, where P is the crack growth parameter and A and b are material constants. By integrating the power law crack growth expression, Swanson et al.[1] showed that the Coffin–Manson exponent m was identical to the power law crack growth exponent b. Likewise, Mowbray[2] showed that a J-integral approach for crack growth reduces to a Coffin–Manson relation for fully reversed cyclic loading cases. These conclusions in combination with the successful application of crack growth type parameters to TMF crack modeling obtained by Nissley et al.[3] and Heine et al.[4] indicate that a suitable crack growth parameter can be found to predict both TMF crack initiation and mode I crack growth.

Theory

A literature search of crack growth models capable of modeling crack initiation was completed. Existence of such models was indicated by Weerasooriya et al.[5] in their review of nonlinear fracture mechanics fatigue models. In that review, a J integral approach based on the work of Rice,[6] Dowling and Begley,[7] Dowling,[8,9] and El Haddad et al.[10] correlated both short and long crack growth behavior of A533B steel. The growth rate of short cracks was captured by an effective crack length $(l + l_0)$ where l_0 was considered to be a measure of reduced flow resistance in surface grains due to lack of constraint.[10] The proposed elastic stress

intensity factor was $K_I = \beta\Delta\sigma\sqrt{\pi(l+l_0)}$. The J-integral was then described by

$$\Delta J = \Delta J_e + \Delta J_p \tag{1}$$

$$\Delta J_e = \Delta K_1^2/E = 2\pi(l+l_0)W_e \tag{2}$$

$$\Delta J_p = 2\pi(l+l_0)f(n)W_p \tag{3}$$

where the function $f(n)$ was given by Shih and Hutchinson[11] as a function of the strain hardening exponent n.

Verification of strain-energy-based cracking models for high-temperature isothermal fatigue and TMF was provided by several investigators (e.g., Refs. 12–15). Subsequently, an effective J-integral was developed for TMF crack life prediction of turbine gas path superalloys. The effective J-integral is an empirical strain energy density crack growth parameter and is not a rigorous fracture mechanics parameter.

The effective J-integral TMF cracking model was developed from Eqs. (1–3) and incorporated into a power law form. No distinction is made between crack initiation and crack growth. All TMF cracking is modeled as crack growth. The contribution to TMF cracking caused by plastic energy was modeled by using the tensile inelastic hysteretic energy.[4,16] Modifications to the effective J-integral were considered based on TMF cracking observations and practical limitations.

1) Crack initiation and arrest attributed to grain boundary interactions[17–19] was considered not relevant for the intended TMF life regime (1,000–20,000 cycles).

2) A threshold energy term was incorporated based on TMF life data of PWA 1480[3] and MAR–M509[20].

3) Crack opening/closure effects[21–23] were disregarded due to lack of TMF data, even though crack closure may be linked to the threshold stress intensity.[24,25]

4) The effect of thermal exposure (e.g., oxidation) was incorporated based on observations and conclusions on TMF behavior of many superalloys.[3,4,26–32]

5) A strain energy correction term for nickel-based single crystal anisotropy, f, was developed based on PWA 1480 TMF data.[3] This correction was necessary to correlate crystalline orientation effects.

The developed effective J-integral fracture mechanics TMF model is summarized as follows:

$$\frac{da}{dN} = A J_{\text{eff}} \nu^c \tag{4}$$

$$J_{\text{eff}} = \pi(a+a_0)\left(\beta^2 f W_{\text{eff}}^{\text{tot}}\right)^b - J_{\text{th}} \tag{5}$$

$$W_{\text{eff}}^{\text{tot}} = 2W_e + \alpha W_p \tag{6}$$

$$W_e = (\sigma_{\max} - m\sigma_{\min})^2/2E_{\max}$$
$$m = 1 \quad \text{if} \quad \sigma_{\min} > 0$$
$$m = 0 \quad \text{if} \quad \sigma_{\min} \le 0 \tag{7}$$

$$W_p = \int^{\text{cycle}} \sigma\, d\varepsilon^{\text{in}} \text{ where } \sigma > 0 \tag{8}$$

$$f = f_{\langle 111\rangle}(E_{\max}/E_{\langle 111\rangle})^2 \tag{9}$$

$$1/\nu = \int^{\text{cycle}} \exp[Q_0(1/T_0 - 1/T)]dt \tag{10}$$

where A, b, c, a_0, α, J_{th}, Q_0, and T_0 are material constants. The constant α in combination with the crack-boundary-correction factor β replaces $f(n)$ in Eq. (3). The threshold J-integral, J_{th}, may be constant or temperature dependent. A good empirical temperature-dependent formula for J_{th} is

$$J_{\text{th}} = J_0 \exp[Q_0(1/T_{\max} - 1/T_J)] \text{ for } T_{\max} \ge T_J \tag{11}$$

where T_J is the temperature below which $J_{\text{th}} = J_0$. All model constants are independent of temperature. The effects of cyclical temperature excursions is captured by Eqs. (10) and (11) and the natural variation in $\sigma_{\max}$ caused by temperature level.

Note that Eqs. (4) and (5) depart from a traditional power law crack growth formulation in that the exponent b is not applied to the J-integral, J_{eff}. Instead, the exponent b is applied to the term $(\beta^2 W_{\text{eff}}^{\text{tot}})$. This departure was necessary to correlate the observed TMF cracking behavior of high-strength superalloys such as PWA 1480. In elastic cases where the exponent $b = 1$, Eqs. (4) and (5) reduce to a traditional Paris law crack growth formula with an exponent of 2.

The TMF life model formulation is limited to transgranular cracking. Another material constant, term, or model is required to capture intergranular TMF cracking behavior. Such is the case for TMF crack growth of B1900+Hf.[33] B1900+Hf integranular crack growth is significantly more rapid than transgranular crack growth at identical effective J-integral levels.

The TMF life model can capture multiaxial effects by using a maximum principle stress based effective J-integral approach. Essentially, stresses and inelastic strains are replaced by normal stresses and inelastic strains along the maximum principle stress direction.

Constant Determination

TMF model material constants are determined from a combination of uniaxial TMF and oxidation tests. The material constants are determined by applying a nonlinear least squares regression analysis. However, estimates of most constants can be determined as follows: For constants b and α, manually adjust α to correlate TMF life of nondwell, low $T_{\max}$ tests using $W_{\text{eff}}^{\text{tot}}$ where $\alpha = 1$ is a good starting point. For polycrystalline materials $a_0 \approx \frac{1}{4}$ grain size and for single crystal materials $a_0 \approx$ microdefect size. For Q_0 fit the Arrhenius equation to oxidation data[34] where $\delta = \{\exp[Q_0(1/T - 1/T_{\text{ox}})]t\}^n$ and where T_{ox} and n are constants and t is time. For polycrystalline materials $T_0 \approx 0.8$–$0.9\ T_{\text{melt}}$, and for single crystal materials $T_0 \approx 0.9$–$1.0\ T_{\text{melt}}$ where T_{melt} is the incipient melting absolute temperature. T_J is the temperature at which time-dependent deformation (creep) becomes significant in monotonic tensile tests (about 750 to 850°C). For uncoated material $c \approx 0.5$ and for coated materials $c \approx 0.1$–0.5 depending on the coating oxidation resistance.

Application

TMF model prediction capability was determined using uncoated MAR-M509 and overlay coated PWA 1480. MAR-M509 is a conventionally cast cobalt superalloy generally used in static turbine airfoil and blade tip seal applications. Its microstructure consists of dispersed MC carbides in a solid solution matrix. PWA 1480 is a nickel-based single crystal superalloy comprised of a high-volume fraction (approximately 65%) of gamma prime pricipitate in a gamma matrix. Its properties offer greater creep-fatigue resistance at elevated temperatures and reduced susceptibility to corrosion and oxidation than conventional cast superalloys. PWA 1480 was the first single crystal extensively used for rotating turbine airfoils.

Elastic and plastic strain energy densities were obtained from nonlinear finite element analyses using Walker's unified viscoplastic model.[3,35] Crack-boundary-correction factors were determined from Newman and Raju[36] for part-through cracks and from Murthy et al.[37] for circumferential-through cracks. Newman and Raju's K solution correlation duplicated Delale and Erdogan's[38] cylindrical shell solution within the specified solution accuracy (about 10%). The circumferential crack-boundary-correction factor included an empirical correction for the shape of the crack front that was developed from observations of tubular specimens. The following formulas were used to correct for the crack front shape (see Fig. 1 for parameter definitions):

$$\theta_0 = \sin^{-1}(c_{\text{proj}}/r_0) \tag{12}$$

$$\theta_i = \big(1.0732 - 3.9888\theta_0 + 12.392\theta_0^2 - 15.419\theta_0^3 + 8.998\theta_0^4 - 2.0463\theta_0^5\big)\theta_0 \tag{13}$$

$$c_m = (r_i + r_0)(\theta_i + \theta_0)/4 \tag{14}$$

where c_m is an estimate of the circumferential half-crack length at the mean radius of the tube wall. The stress intensity for circumferential cracks was based on c_m.

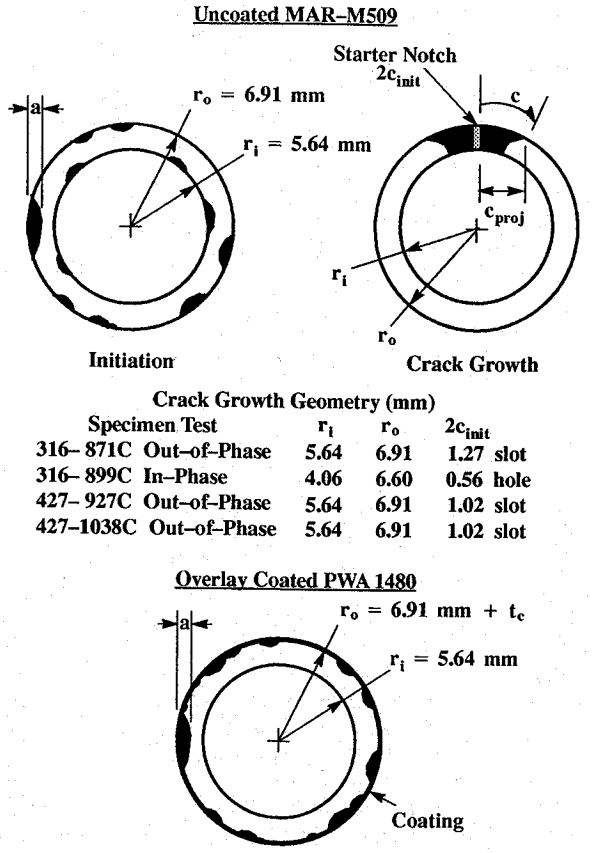

Crack Growth Geometry (mm)

Specimen	Test	r_i	r_o	$2c_{init}$
316–871C	Out-of-Phase	5.64	6.91	1.27 slot
316–899C	In-Phase	4.06	6.60	0.56 hole
427–927C	Out-of-Phase	5.64	6.91	1.02 slot
427–1038C	Out-of-Phase	5.64	6.91	1.02 slot

Fig. 1 TMF specimen and typical crack geometries.

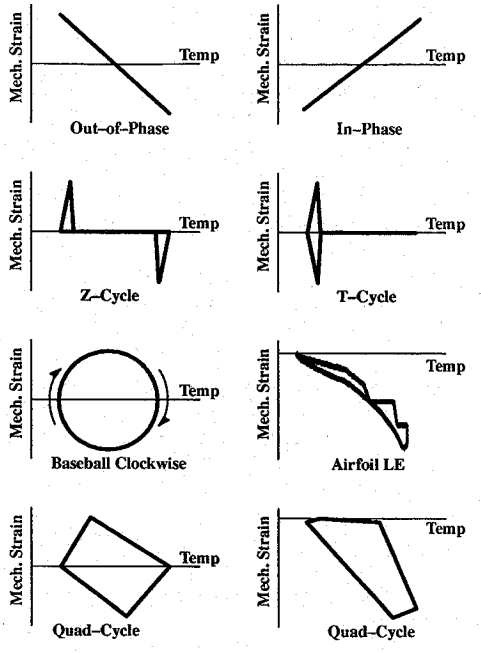

Fig. 2 TMF strain-temperature cycle schematics.

Test procedures and metallurgical observations are presented in Refs. 3, 4, and 20. TMF specimen and typical crack geometries are presented in Fig. 1 and Ref. 20. TMF tests were run at least until crack initiation and most were run to failure.

Most TMF tests were conducted using an out-of-phase mechanical strain-temperature ($\varepsilon - T$) relationship, but a few tests were run with more complex $\varepsilon - T$ cycles to challenge model prediction capability. TMF $\varepsilon - T$ cycles are presented in Fig. 2. All cycles were run at 1 cycle/min (cpm) unless noted otherwise in the figures.

The TMF model was applied by assuming that a single dominant crack controls the TMF life. Typically, many cracks were observed along the surface(s) of the specimens as shown in Fig. 1. Multiple cracks were especially prevalent in the overlay coated PWA 1480 TMF specimens. However, calculation along multiple crack fronts was considered too complex for initial model development.

Uncoated MAR-M509

MAR-M509 has been studied by many investigators.[20,39–44] TMF cracking of MAR-M509 was observed along preferentially oxidized carbides and was generally transgranular in nature. TMF life data were segregated into two data sets: Ref. 20 data and Pratt and Whitney (P&W) data. TMF specimen cyclic history was predicted using a unified viscoplastic model[35] correlated to MAR-M509 monotonic tensile and Ref. 20 TMF specimen data. The MAR-M509 viscoplastic model was executed until a stabilized hysteresis loop was predicted. TMF model material constants were determined using predicted stabilized hysteresis loop behavior. The constant Q_0 was determined from cyclic oxidation burner rig data, and the constant c was set to 0.5 based on matrix oxidation rate data[41]. The remainder of the model constants were determined by nonlinear least-squares-regression analysis of the Ref. 20 TMF data. Model constants A and T_0 were then adjusted to correlate the P&W TMF data set. Model correlation capability is presented in Fig. 3 and model constants are presented in Table 1. Within a particular data set, the model correlates the observed TMF life within a factor of $\pm 2X$. However, the Ref. 20 and P&W data life correlations are different by about $2X$.

The cause of the calculated life difference between the two data sets is not known, but it may be related to microstructure. The specimen grain size of both data sets was about equal. However, the Ref. 20 specimens were heat treated 6 h at 1230°C prior to testing. The heat treatment produced MC carbides which have been linked to increased crack growth rate.[44] The P&W specimens were not similarly heat treated. The higher value of T_0 obtained for the P&W data is consistent with the microstructural argument.

Model predictive capability was assessed by applying the correlated model to a variety of uncoated TMF crack growth tests such as those described by Rau et al.[39] The Rau et al.[39] Mar-M509 material was similar to the P&W material used in the TMF model constant determination process. Figure 4 presents the model predictions. In general, the model was able to predict crack growth life up to projected half-crack sizes, c_{proj}, of about 1.27 mm within a factor of $2X$. Beyond a 1.27-mm half-crack size, the model over-predicts the crack growth life. Nonetheless, a significant portion of the TMF crack growth life was well predicted.

In all but one crack growth test, the TMF hysteresis loop behavior was predicted to stabilize within a few cycles by nonlinear stress

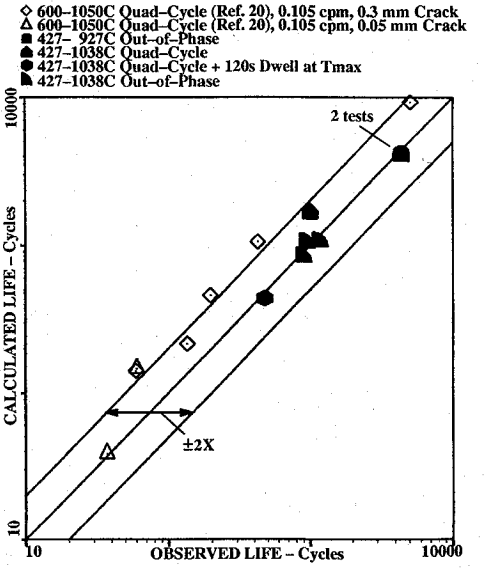

Fig. 3 TMF model correlation of uncoated MAR-M509 TMF life.

Table 1 Summary of TMF life model constants

	A, m/cycle (in/cycle)	b	c	a_0, m (in.)	α	J_{th}, N/m (lbf/in.)	J_0, N/m (lbf/in.)	T_J, K(°R)	Q_0, K(°R)	T_0 K(°R)
MAR–M509 (Ref. 20)	1.7388×10^{-5}	1.0	0.5	1.8964×10^{-4}	1.0	8.979×10^{-2}	—	—	35,247	1,273
	(3.0453×10^{-6})			(7.3600×10^{-3})		(5.127×10^{-1})			(63,600)	(2,260)
MAR–M509 (P&W)	1.5172×10^{-5}	1.0	0.5	1.8964×10^{-4}	1.0	8.979×10^{-2}			35,247	1,300
	(2.6571×10^{-6})			(7.3600×10^{-3})		(5.127×10^{-1})	—	—	(63,600)	(2,340)
Overlay coated PWA 1480	0.002794 (0.11)	1.0	0.15	2.540×10^{-5} (0.001)	10.0	—	5.867×10^{-3} (0.231)	1144 (2,060)	29,722 (53,500)	1,575 (2,835)

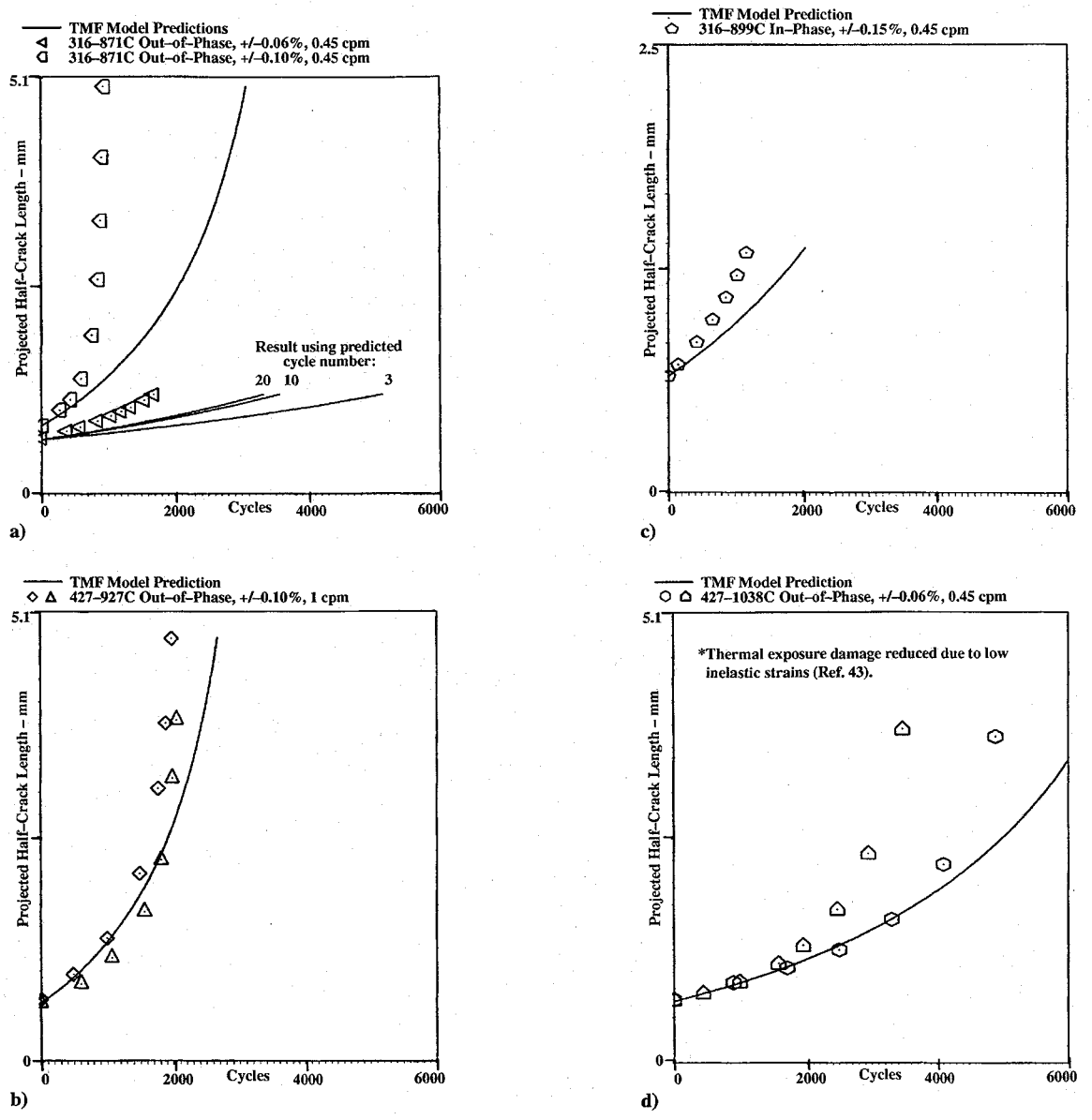

Fig. 4 TMF model predictions of uncoated MAR-M509 TMF crack growth.

analysis. However, as shown in Fig. 4a, sometimes many cycles were needed to stabilize the hysteresis behavior. In this case, additional cycle predictions were needed to ratchet the hysteresis loop into tension until compressive creep plasticity was completely reversed by tensile plasticity. Thus, TMF models based on nonlinear stress analyses of turbine components must be carefully implemented to avoid life prediction inaccuracies caused by nonstabilized hysteresis loop predictions.

Overlay Coated PWA 1480

Based on previous rig[3,4] and gas turbine engine experience,[27] it was concluded that coatings have a role equally important with that of the substrate superalloy in determining turbine component TMF cracking life. Coatings, applied to the component surfaces to provide oxidation protection, served as the primary TMF crack initiation site at turbine operating conditions. Coating TMF cracks act as initial flaws for substrate TMF crack growth.

PWA 1480 is a single crystal material. Its elastic modulus is highly dependent on crystallographic orientation.[3,4] To capture TMF cracking in PWA 1480 by a strain energy density parameter requires incorporation of a crystallographic factor. The crystallographic factor is needed to alter the elastic modulus used in calculating the elastic strain energy density. To be effective, the factor must suppress the crystallographic orientation effect on elastic modulus. The crystallographic factor developed by Nissley et al.[3] [Eq. (9)] suppresses the elastic modulus dependency on crystallographic orientation by

partitioning the strain energy density. The strain energy density portion considered damaging is associated with the maximum normal stressed octahedral slip plane. This is based on the notion that mode I TMF cracking of PWA 1480 occurs on a microscopic level along the maximum normal stressed octahedral slip plane. Metallurgical evaluation of PWA 1480[4] indicates that octahedral slip plane cracking occurs in some TMF cases, but whether such activity dominates TMF crack growth in all cases is not known. However, metallurgical evaluation of high-strain TMF tests of single crystal superalloy CMSX-6[45] indicates that octahedral slip plane cracking does dominate the low life regime (< 1000 cycles).

Unlike MAR-M509, PWA 1480 TMF cycling is virtually elastic within the relevant life regime.[3,20] However, monotonic creep (stress relaxation) occurs during the high-temperature portion of the cycle which ratchets the hysteresis loop stress into tension or compression depending on the $\varepsilon - T$ cycle. Such ratcheting behavior dramatically alters the elastic strain energy density during the TMF life of the material. Thus, strain energy densities were obtained by empirically scaling nonlinear finite element analysis predictions of initial hysteresis loop behavior to stable conditions. The hysteresis loop scaling method is too lengthy to fully describe herein, but it essentially is based on the observed relationship between the maximum temperature stabilized stress of ⟨001⟩ out-of-phase TMF specimen tests and ⟨001⟩ 0.2% yield stress obtained at the TMF test maximum temperature. Stable conditions were assumed to occur at one-half of the specimen failure life. TMF model application to turbine hardware is accomplished by scaling the maximum principle stress direction hysteresis loop. In all cases the plastic strain energy density was zero or very small in comparison to the elastic strain energy density. The nonlinear analyses were conducted using a revised form of the Ref. 3 micromechanistic single crystal formulation correlated to isothermal tensile test data. The viscoplastic model revision eliminated the equilibrium stress state variable to improve hysteresis loop stress relaxation behavior predictions and facilitate hysteresis loop scaling. Since cycling of PWA 1480 is virtually elastic in the relevant life regime, elimination of the equilibrium stress was considered a good engineering approximation.

TMF model constants were determined by nonlinear least-squares regression. The maximum stress used in the regression analysis was either the predicted initial cycle tensile stress or the predicted (scaled) stabilized cycle tensile stress, whichever was greater. Coated PWA 1480 life was defined as the number of TMF cycles to either PWA 1480 crack initiation (N_{sc}) or PWA 1480 failure ($N_{sc} + N_{sp}$) by using the following relationship:

$$N_f - N_c = N_{sc} + N_{sp} \tag{15}$$

Acetate film crack replica data and TMF specimen loads were used to determine N_{sc}.[3] Because a coating was present, the initial defect size in Eq. (5) was set to the sum of coating thickness t_c and a_0 (i.e., $a + a_0$ was replaced by $a + a_0 + t_c$). Thicker coatings increase the initial PWA 1480 effective crack size which raises the initial stress intensity and lowers TMF life. PWA 1480 TMF specimen coating thicknesses ranged from 0.025 to 0.381 mm with a nominal thickness of 0.127 mm. Coating modulus was about 30% higher than PWA 1480 at the maximum tensile stress temperature. The effect of coating modulus on PWA 1480 initial stress intensity was not included in the model. Best correlation results were obtained when the material constant A was divided by the 0.2% offset yield strength of ⟨001⟩ oriented tensile specimens. The ⟨001⟩ orientation 0.2% yield strength value was determined at the specimen maximum temperature and was determined for each TMF specimen individually. The correlation data set used to determine TMF model constants consisted of failure and crack initiation (0.254-mm-deep PWA 1480 crack) TMF life data from ⟨001⟩ and ⟨213⟩ crystallographically oriented test specimens. The ⟨213⟩ specimen data was needed to help determine the effects of thermal exposure (dwell time) because sufficient ⟨001⟩ dwell time specimen data was not available. The correlation data fit is presented in Fig. 5 and the model constants are presented in Table 1. Failure life was correlated within $\pm 2X$, and the crack initiation life was correlated within $\pm 2.5X$. The calculated crack initiation lives averaged slightly higher than the observed crack initiation lives. Poorer correlation of the crack initiation data

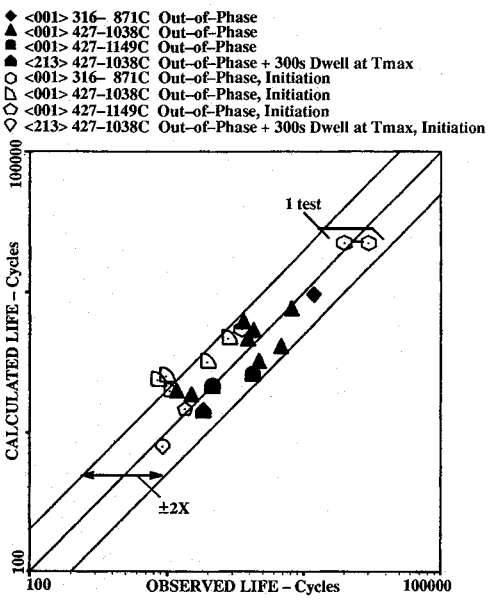

Fig. 5 TMF model correlation of overlay coated PWA 1480 TMF life.

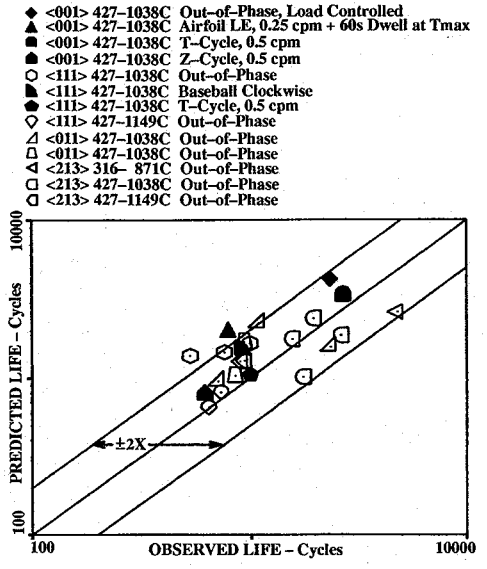

Fig. 6 TMF model prediction of overlay coated PWA 1480 TMF crack initiation life.

may be caused by a combination of effects such as 1) the assumption that no TMF damage occurred in the PWA 1480 until coating cracks reached the coating—PWA 1480 interface (in some cases, particularly the high modulus single crystal orientations, several thousand cycles were run before the coating was cracked, 2) the influence of the coating on PWA 1480 small crack stress intensity, 3) the difficulty in precisely determining crack depth in coated specimens from acetate film replication of surface cracks,[3] and 4) the influence of multiple fatigue cracks. These effects limit the PWA 1480 TMF model presented to overlay coated situations. Different model constants are required to predict aluminide coated or uncoated PWA 1480 TMF life.

Overlay coated PWA 1480 TMF life model predictive capability was assessed using crack initiation and failure life data from specimens with various overlay coatings, crystallographic orientations, $\varepsilon - T$ cycles and loading types. The predictions are presented in Figs. 6 and 7. The crack initiation life data are slightly overpredicted, but the predictions are still within $\pm 2.5X$, consistent with the correlation data set. The failure life data are predicted within about $\pm 2X$. Overall, the TMF model provided a good estimate of TMF crack initiation and mode I crack growth in overlay coated PWA 1480.

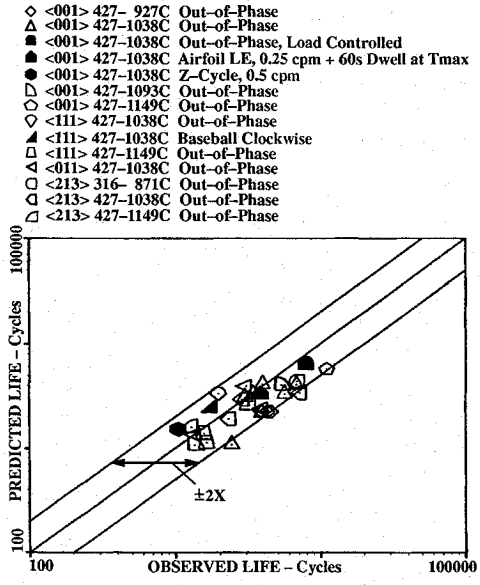

Fig. 7 TMF model prediction of overlay coated PWA 1480 TMF failure life.

Conclusions

TMF crack initiation and mode I crack growth of uncoated MAR-M509 and overlay coated PWA 1480 can be adequately predicted by using a thermal exposure modified effective J-integral fracture mechanics model. The model can capture many TMF cracking effects such as coating thickness, single crystal anisotropy, cycle wave-shape, dwell, and thermal exposure. Good estimates of TMF model constants can be obtained from limited uniaxial TMF tests.

Unified viscoplastic constitutive models provide a good description of initial TMF stress-strain hysteresis loop behavior. For low yield strength superalloys, the stress-strain hysteresis quickly stabilizes and initial viscoplastic model predictions are adequate. However, high-strength superalloy TMF hysteresis loop behavior evolves over hundreds or thousands of cycles. In such cases, initial viscoplastic model TMF cycle predictions must be scaled to stabilized conditions to obtain the appropriate stresses for TMF modeling.

References

[1]Swanson, G. A., Linask, I., Nissley, D. M., Norris, P. P., Meyer, T. G., and Walker, K. P., "Life Prediction and Constitutive Models for Engine Hot Section Anisotropic Materials Program, Second Annual Report," NASA CR-179594, April 1987.

[2]Mowbray, D. F., "Derivation of a Low-Cycle Fatigue Relationship Employing the J-Integral Approach to Crack Growth," *Cracks and Fracture*, ASTM STP 601, American Society for Testing and Materials, 1976, pp. 33–46.

[3]Nissley, D. M., Meyer, T. G., and Walker, K. P., "Life Prediction and Constitutive Models for Engine Hot Section Anisotropic Materials Program, Final Report," NASA CR-189223, Sept. 1992.

[4]Heine, J. E., Warren, J. R., and Cowles, B. A., "Thermal Mechanical Fatigue of Coated Blade Materials, Final Report," Wright Research Development Center-TR-89-4027, Wright–Patterson AFB, OH, June 1989.

[5]Weerasooriya, T., Gallagher, J. P., and Rhee, H. C., "A Review of Nonlinear Fracture Mechanics Relative to Fatigue," Air Force Weapons Lab., AFWL-TR-79-4196, Wright–Patterson AFB, OH, Dec. 1979.

[6]Rice, J. R., "A Path Independent Integral and the Approximate Analysis of Strain Concentration by Notches and Cracks," *Journal of Applied Mechanics*, Vol. 35, 1968, pp. 379–386.

[7]Dowling, N. E., and Begley, J. A., "Fatigue Crack Growth During Gross Plasticity and the J-Integral," *Mechanics of Crack Growth*, ASTM STP 590, American Society for Testing and Materials, Philadelphia, PA, 1976, pp. 82–103.

[8]Dowling, N. E., "Geometry Effects and the J-Integral Approach to Elastic-Plastic Fatigue Crack Growth," *Cracks and Fracture*, ASTM STP 601, American Society for Testing and Materials, Philadelphia, PA, 1976, pp. 19–32.

[9]Dowling, N. E., "Crack Growth During Low-Cycle Fatigue of Smooth Axial Specimens," *Cyclic Stress-Strain and Plastic Deformation Aspects of Fatigue Crack Growth*, ASTM STP 637, American Society for Testing and Materials, Philadelphia, PA, 1977, pp. 97–121.

[10]El Haddad, M. H., Smith, K. N., and Topper, T. H., "Fatigue Crack Propagation of Short Cracks," *Journal of Engineering Materials and Technology*, Vol. 101, Jan. 1979, pp. 42–46.

[11]Shih, C. F., and Hutchinson, J. W., "Fully Plastic Solutions and Large Scale Yielding Estimating for Plane Stress Crack Problems," Div. of Engineering and Applied Physics, Rept. DEAP-S-14, Harvard Univ., Cambridge, MA, July, 1975.

[12]Pelloux, R. M., and Ramanoski, G. R., "A Study of the Fatigue Behavior of Small Cracks in Powder Metallurgy IN100 at 649°C," U.S. Air Force Office of Scientific Research and Pratt & Whitney Aircraft Group; work done at Massachusetts Institute of Technology, Oct. 1988.

[13]Sadananda, K., and Shahinian, P., "A Fracture Mechanics Approach to High Temperature Fatigue Crack Growth in Udimet 700," *Engineering Fracture Mechanics*, Vol. 11, 1979, pp. 73–86.

[14]Jordan, E. H., and Meyers, G. J., "Fracture Mechanics Applied to Elevated Temperature Fatigue Crack Growth," *Journal of Engineering Materials and Technology*, Vol. 111, July 1989, pp. 306–313.

[15]Hill, J. T., "Thermomechanical Fatigue Crack Growth (TMFCG) in Fine Grained Precipitation Aged Alloy PWA 1455," Memo to G. A. Swanson, Pratt & Wihtney, E. Hartford, CT, Feb. 20, 1986.

[16]Ostergren, W. J., "A Damage Function and Associated Failure Equations for Predicting Hold Time and Frequency Effects in Elevated Temperature Low-Cycle Fatigue," *Journal of Testing and Evaluation*, Vol. 4, No. 5, 1976, pp. 327–339.

[17]Miller, K. J., "Initiation and Growth Rates of Short Fatigue Cracks," *Conference Proceedings on Fundamentals of Deformation and Fracture*, Eshelby Memorial Symposium, Univ. of Sheffield, 1984, pp. 477–500. Cambridge Univ. Press, Cambridge, England, UK.

[18]Davidson, D. L., and Lankford, J., "Experimental Mechanics of Fatigue Crack Growth: The Effect of Crack Size," *Conference Proceedings on Fundamentals of Deformation and Fracture*, Eshelby Memorial Symposium, Univ. of Sheffield, Cambridge Univ. Press, Cambridge, England, UK, 1984, pp. 559–572.

[19]Sun, Z., De Los Rios, E. R., and Miller, K., "Modelling Small Fatigue Cracks Interacting with Grain Boundaries," *Fatigue and Fracture of Engineering Materials and Structures*, Vol. 14, No. 2/3, 1991, pp. 277–291.

[20]François, M., and Rémy, L., "Thermal-Mechanical Fatigue of MAR-M509 Superalloy, Comparison with Low-Cycle Fatigue Behavior," *Fatigue and Fracture of Engineering Materials and Structures*, Vol. 14, No. 1, 1991, pp. 115–129.

[21]Newman, J. C., "A Crack Opening Stress Equation for Fatigue Crack Growth," *International Journal of Fracture*, Vol. 24, 1984, pp. R131–R135.

[22]May, I. L., and Cheung, S. K. P., "Closure Effects in Short and Long Fatigue Cracks," Proceedings of the 6th International Conf. on Fracture, *Advances in Fracture Research, Fracture 84*, Vol. 3, pp. 1903–1910. Pergamon, New York.

[23]McEvily, A. J., and Yang, Z., "On the Significance of Crack Closure in Fracture Crack Growth," Proceedings of the 7th International Conf. on Fracture, *Advances in Fracture Research*, Pergamon, New York, Vol. 2, 1989, pp. 937–944.

[24]Anderson, T. L., *Fracture Mechanics: Fundamentals and Applications*, CRC Press, Boca Raton, FL, 1991.

[25]McEvily, A. J., and Minakawa, K., "On the Significance of the Threshold for Fatigue Crack Growth," Proceedings of the 6th International Conf. on Fracture, *Advances in Fracture Research, Fracture* 84, Pergamon, New York. Vol. 3, 1984, pp. 1641–1647.

[26]Malpertu, J. L., and Rémy, L., "Thermal-Mechanical Fatigue Behavior of IN100 Superalloy," Proceedings of a Conf. Liège, Belgium, *High Temperature Alloys for Gas Turbines and Other Applications*, D. Reidel, Boston, MA. 1986, pp. 1559–1568.

[27]Bernstein, H. L., and Allen, J. M., "Analysis of Cracked Gas Turbine Blades," American Society of Mechanical Engineers, ASME 91-GT-16, June, 1991.

[28]Neu, R. W., and Sehitoglu, H., "Thermomechanical Fatigue, Oxidation, and Creep: Part 1, Damage Mechanisms," *Metallurgical Transactions*, Vol. 20A, Sept. 1989, pp. 1755–1767.

[29]Boismier, D. A., and Sehitoglu, H., "Thermomechanical Fatigue of MAR-M247: Part 1—Experiments," *Journal of Engineering Materials and Technology*, Vol. 112, Jan. 1990, pp. 68–79.

[30]Sehitoglu, H., and Boismier, D. A., "Thermomechanical Fatigue of MAR-M247: Part 2—Life Prediction," *Journal of Engineering Materials and Technology*, Vol. 112, Jan. 1990, pp. 80–89.

[31]Boone, D. H., and Sullivan, C. P., "Effect of Several Metallurgical Variables on the Thermal Fatigue Behavior of Superalloys," *Fatigue at Elevated Temperature*, ASTM STP 520, American Society for Testing and Materials, Philadelphia, PA, 1973, pp. 401–415.

[32]Nelson, R. S., Levan, G. W., and Schoendorf, J. F., "Creep Fatigue Life Prediction for Engine Hot Section Materials (Isotropic), Second Interim Report," NASA CR-189220, Aug. 1992.

[33]Marchand, N., and Pelloux, R. M., "Thermal-Mechanical Fatigue Crack Growth in B-1900+Hf," Proceedings of Conf. Liège, Belgium, *High Temperature Alloys for Gas Turbines and Other Applications*, D. Reidel, Boston, MA, 1986, pp. 1547–1558.

[34]Meier, S. M., Nissley, D. M., Sheffler, K. D., and Cruse, T. A., "Thermal Barrier Coating Life Prediction Model Development," ASME 91-GT-40, American Society of Mechanical Engineering, June 1991.

[35]Walker, K. P., "Research and Development Program for Nonlinear Structural Modeling with Advanced Time-Temperature Dependent Constitutive Relationships," NASA CR-165533, Nov. 1981.

[36]Newman, J. C., and Raju, I. S., "Stress-Intensity Factor Equations for Cracks in Three-Dimensional Finite Bodies Subjected to Tension and Bending Loads," NASA TM-85793, April, 1984.

[37]Murthy, M. V. V., Rao, K. P., and Rao, A. K., "On the Stress Problem of Large Elliptical Cutouts and Cracks in Circular Shells, *International Journal of Solids and Structures*, Vol. 10, 1974, pp. 1243–1269.

[38]Delale, F., and Erdogen, F., "Application of the Line-Spring Model to a Cylindrical Shell Containing a Circumferential or Axial Part—Through Crack," *Journal of Applied Mechanics*, Vol. 49, March 1982, pp. 97–102.

[39]Rau, C. A., Gemma, A. E., and Leverant, G. R., "Thermal-Mechanical Fatigue Crack Propagation in Nickel-and Cobalt-Base Superalloys Under Various Strain-Temperature Cycles," *Fatigue at Elevated Temperatures*, ASTM STP 520, 1973, American Society for Testing and Materials, Philadelphia, PA, pp. 166–178.

[40]François, M., and Rémy, L., "Influence of Microstructure on the Thermal Fatigue Behavior of a Cast Cobalt-Base Superalloy," *Metallurgical Transactions*, Vol. 21A, April, 1990, pp. 949–958.

[41]Reger, M., and François, M., and Rémy, L., "Interaction Between Oxidation and Cyclic Straining at High Temperature," *Physical Chemistry of the Solid State: Applications to Metals and Their Compounds*, Elsevier Science, New York, 1984, pp. 413–420.

[42]Reger, M., Rezai Aria, F., and Rémy, L. "Low Cycle Fatigue Propagation of Microcracks in Two Superalloys," Proceedings of the 6th International Conf. on Fracture, *Advances in Fracture Research, Fracture 84*, Pergamon, New York, Vol. 3, 1984, pp. 1589–1595.

[43]Fischmeister, H. F., Danzer, R., and Buchmayr, B., "Life Time Prediction Models," Proceedings of Conf. Liège, Belgium, *High Temperature Alloys for Gas Turbines and Other Applications*, D. Reidel, Boston, MA, 1986, pp. 495–549.

[44]Beck, C. G., and Santhanam, A. T., "Effect of Microstructure on the Thermal Fatigue Resistance of a Cast Cobalt-Base Alloy, Mar-M509," *Thermal Fatigue of Materials and Components*, ASTM STP 612, American Society for Testing and Materials, Philadelphia, PA, 1976, pp. 123–140.

[45]Kraft, S., Zauter, R., and Mughrabi, H., "Aspects of High-Temperature Low-Cycle Thermomechanical Fatigue of a Single Crystal Nickel-Base Superalloy," *Fatigue and Fracture of Engineering Materials and Structures*, Vol. 16, No. 2, 1993, pp. 237–253.